Molecular Crystals and Liquid Crystals
Publication details, including instructions for authors and subscription information:
http://www.tandfonline.com/loi/gmcl20

# Electro-Optical Properties of Polymer Dispersed Liquid Crystal Transmission Gratings

Mojca Jazbinšek [a], Irena Drevenšek Olenik [a], Marko Zgonik [a], Adam K. Fontecchio [b] & Gregory P. Crawford [b]

[a] Department of Physics, University of Ljubljana, J. Stefan Institute, Jamova 39, Ljubljana, SI-1001, Slovenia

[b] Department of Physics, Brown University, Providence, Rhode Island, 02912

Version of record first published: 18 Oct 2010

To cite this article: Mojca Jazbinšek, Irena Drevenšek Olenik, Marko Zgonik, Adam K. Fontecchio & Gregory P. Crawford (2002): Electro-Optical Properties of Polymer Dispersed Liquid Crystal Transmission Gratings, Molecular Crystals and Liquid Crystals, 375:1, 455-465

To link to this article: http://dx.doi.org/10.1080/713738362

*Mol. Cryst. Liq. Cryst.*, Vol. 375, pp. 455-465

1058-725X/02 $12.00 + .00



# Electro-Optical Properties of Polymer Dispersed Liquid Crystal Transmission Gratings

MOJCA JAZBINŠEK[a], IRENA DREVENŠEK OLENIK[a], MARKO ZGONIK[a], ADAM K. FONTECCHIO[b] and GREGORY P. CRAWFORD[b]

[a]*Department of Physics, University of Ljubljana, and J. Stefan Institute, Jamova 39, SI-1001 Ljubljana, Slovenia and*
[b]*Department of Physics, Brown University, Providence, Rhode Island 02912*

We report on the investigations of electrically switchable polymer dispersed liquid crystal gratings. Diffraction properties, grating anisotropy, and temperature dependencies were analyzed to obtain information on the liquid crystal orientation inside the ellipsoidal droplets and the distribution of the droplets in a polymer host. We compare the samples of different compositions and grating spacings.

Keywords: H-PDLC; holographic gratings; polymer dispersed liquid crystals; switchable gratings; nematic director structure in ellipsoidal voids

## INTRODUCTION

Holographic polymer dispersed liquid crystals (H-PDLCs) are the subject of extensive studies due to a variety of possible applications, including flat-panel displays and optical switches. These liquid crystal (LC)/polymer composite materials consist of alternating layers of homogeneous polymer planes and LC rich droplet planes. H-PDLC materials are attractive for electrically switchable holographic gratings since the diffraction efficiency can be dynamically controlled by external voltages. An external electric field reorients LC molecules in the

droplets and thus changes the optical properties of the grating.

H-PDLCs are made from a mixture of photosensitive monomers and LC which is exposed to two interfering laser beams. In bright regions the polymerization occurs more rapidly than in dark regions and LC diffuses to dark regions. Owing to the phase separation, the refractive index of the system is modulated and an optical phase grating is formed. The performance of H-PDLCs is directly connected to their structure, i.e. the distribution of LC droplets in the polymer host, the shape and the size of the droplets, and LC orientation profile within the droplets. The structure parameters differ considerably in different samples, dependent on the components of pre-polymer/LC emulsion and the preparation procedure. Grating morphology studies of transmission gratings showed[1] that the droplet density, size, and shape anisotropy increase with increasing LC concentration. The effect of the functionality (the monomer property that can yield a cross-linked network) on the final diffraction efficiency was examined[2]. The exposure time and the light power density used for grating formation are also important parameters for the grating characteristics. We have recently reported[3] on the diffraction properties, grating anisotropy, electro-optic response, and temperature dependence of transmission H-PDLC gratings cured by visible laser light. In this paper we report on experimental study of the diffraction properties of similar gratings cured by UV laser light and we give comparison of the relevant parameters to those reported previously[3].

## EXPERIMENTAL

Two different material mixtures made of commercially available constituents were used to form the gratings and the details are given in Table 1. We label them as VIS and UV. VIS samples were cured by visible laser beams ($\lambda = 514$ nm) and UV samples by UV laser beams ($\lambda = 351$ nm). The writing beams intersected symmetrically inside the material, so that the produced grating has the grating vector $\boldsymbol{K}_{\mathrm{g}}$ parallel to sample surfaces (Figure 1). Samples of three different grating spacings were made from each mixture. All the samples were 5 $\mu$m thick.

Scanning electron microscopy (SEM) images of VIS samples of different

| Material label | Constituents |
|---|---|
| **VIS** | 32.4% BL038 nematic LC* |
| | 22.5% aliphatic urethane resin oligomer 4866** |
| | 22.5% aliphatic urethane resin oligomer 8301** |
| | 12.6% photoinitiator Rose Bengal, co-initiator N-Phenylglycine and chain-terminator N-Vinyl Pyrrolidinone*** |
| | 10% surfactant S-271 POE sorbitan monooleate**** |
| **UV** | 50% TL203 nematic LC* |
| | 50% PN393 mixture of acrylated monomers and oligomers with photoinitiator* |

* EM Industries ** Ebecryl (Radcure) *** Sigma-Aldrich **** Chem Service

TABLE 1: The components of the pre-polymer and LC emulsion used to prepare our samples.

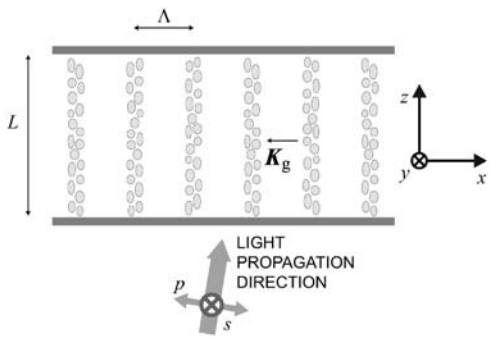


FIGURE 1: Schematic drawing of H-PDLC transmission grating of thickness $L$ and grating spacing $\Lambda$. Planes of LC droplets are separated by regions of polymer. Two orthogonal polarizations $p$ and $s$ of incoming light are illustrated. The coordinate axis $x$ is chosen to be parallel to the grating vector $\boldsymbol{K}_g$ and $y$ parallel to the sample surface. Glass surfaces are coated with indium tin oxide (ITO) electrodes.

grating spacings showed that the droplets take the form of ellipsoids of unequal axes that are squeezed in the direction of the grating vector[3]. The separation between LC and polymer regions was more pronounced for smaller grating

spacings. The contrast of SEM images of UV samples was too low to observe the detailed structure, which is probably due to different properties of the polymer. It was therefore not possible to make any relevant structure comparison between VIS and UV gratings on the basis of SEM. In the following we present measurements of the anisotropy and temperature dependence of the diffraction efficiency which allow us to deduce structural characteristics of the UV gratings despite the lack of their SEM images.

For measurements of diffraction efficiency the sample was mounted on a rotation stage with the rotation axis orthogonal to the grating vector ($y$ axis in Figure 1). A frequency doubled cw Nd-YAG laser with wavelength of 532 nm and a beam diameter of approximately 2 mm was used. The intensity of incident beam was around 100 mWcm$^{-2}$. The input light was either $p$-polarized (in the diffraction plane) or $s$-polarized (perpendicular to the diffraction plane). The diffraction efficiency $\eta$, which is defined as the ratio of the diffracted beam with respect to the sum of the diffracted and directly transmitted beam intensities, was measured with a photodiode.

## RESULTS AND DISCUSSION

### Electro-optical performance

The electrical switching properties of LC droplets in H-PDLC samples are of the greatest interest for applications. We have applied the ac electric field $\boldsymbol{E}$ perpendicularly to the sample surfaces, so that the field induced torque reorients the LC molecules along the $z$ axis. The diffraction efficiencies were measured for $p$- and $s$-polarized light for sample orientation satisfying the Bragg condition

$$2n_{\mathrm{m}}\Lambda \sin\theta_{\mathrm{B}} = \lambda_0, \tag{1}$$

where $n_{\mathrm{m}}$ is the mean refractive index, $\Lambda$ the grating spacing, $\lambda_0$ the wavelength of light in vacuum, and $\theta_{\mathrm{B}}$ the inner Bragg angle with respect to the sample normal.

Figure 2 shows two typical graphs of diffraction efficiencies versus the amplitude of the applied ac field. In the VIS sample, the efficiencies are almost constant by applying low electric fields. In higher fields they continuously de-

crease with increasing electric field and then saturate at values of a few percent. The diffraction at high fields is so low because the polymer refractive index was selected to match the LC ordinary refractive index. The ratio of the efficiencies $\eta_p/\eta_s$ (crosses in Figure 2) in the VIS sample exhibits a prominent maximum around the threshold voltage and then decreases to a constant value in strong fields. The behavior is determined by the structural properties of the composite grating[3]. On the contrary to the VIS samples, the diffraction efficiency of the UV samples is larger for $s-$ than for $p$-polarized light. The switching curves are much smoother, although the switching electric field values are similar. The more gradual reduction of the diffraction efficiency and the reversed polarization sensitivity of the UV samples suggest that the grating structure is different than in the case of VIS samples. The gratings may for example have a broader distribution of droplet sizes or lower anchoring strength between LC and polymer.

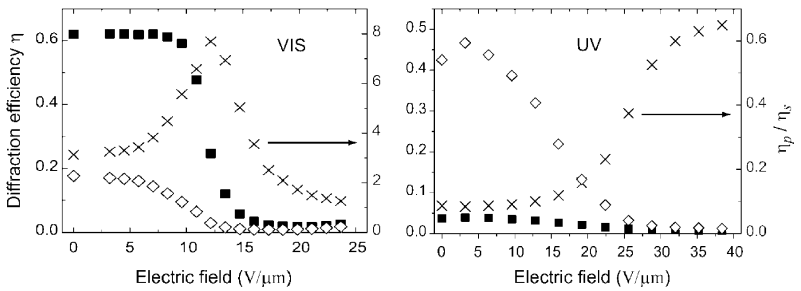


FIGURE 2: The ac electric field ($\nu = 10\,\text{kHz}$) dependence of the diffraction efficiencies $\eta_p$ and $\eta_s$ for the two characteristic samples, VIS sample with $\Lambda = 1.55\,\mu\text{m}$, and UV sample with $\Lambda = 1.2\,\mu\text{m}$, measured at room temperature. Results are shown for $p$-polarization (solid squares), $s$-polarization (open diamonds), and the ratio between them (crosses).

**Grating strength and anisotropy**

In most cases the Bragg diffraction efficiencies measurements with transmission H-PDLCs result in smaller efficiencies for $s$-polarized light[1]. According to the conventional Kogelnik's coupled-wave theory[4], which presumes the scalar refractive index modulation of the grating, the diffraction efficiency for $s$-polarization should always be higher than for $p$-polarization. This is because the coupling between the incident and diffracted wave field components is higher for $s$-waves. The observed opposite behavior of H-PDLCs is a clear evidence that gratings are birefringent and therefore the modified coupled-wave theory[5] should be used to explain the polarization sensitivity[3].

We describe the dielectric tensor of H-PDLCs as being sinusoidally modulated along $x$ axis with the periodicity $\Lambda$. The dielectric tensor is hence given as

$$\boldsymbol{\epsilon}(x) = \boldsymbol{\epsilon}^0 + \boldsymbol{\epsilon}^1 \sin\frac{2\pi x}{\Lambda}, \tag{2}$$

where $\boldsymbol{\epsilon}^0$ is the average dielectric tensor of the composite and $\boldsymbol{\epsilon}^1$ the amplitude of the dielectric tensor modulation. In zero electric field the LC droplets are on the average uniaxial domains and form planes with the symmetry axis in the direction of the grating vector. Hence it follows that tensor $\boldsymbol{\epsilon}^1$ is diagonal with $\epsilon^1_{yy} = \epsilon^1_{zz}$.

For a case of light incident at the Bragg angle, and with small deviation between the energy-propagation and wave-vector directions, the diffraction efficiency of a non-absorptive anisotropic transmission grating is given as[5]

$$\eta = \sin^2\left(\frac{\pi L}{\lambda_0 \cos\theta_\mathrm{B}} \frac{\hat{\boldsymbol{e}}_0 \cdot \boldsymbol{\epsilon}^1 \hat{\boldsymbol{e}}_1}{2n_\mathrm{m}}\right), \tag{3}$$

where $\hat{\boldsymbol{e}}_0$ and $\hat{\boldsymbol{e}}_1$ are the polarization unit vectors for the incident and Bragg reflected beams, and $L$ is the sample thickness. We obtain $\hat{\boldsymbol{e}}_0 \cdot \boldsymbol{\epsilon}^1 \hat{\boldsymbol{e}}_1 = \epsilon^1_{zz}$ for $s$-polarization and $\hat{\boldsymbol{e}}_0 \cdot \boldsymbol{\epsilon}^1 \hat{\boldsymbol{e}}_1 = \epsilon^1_{xx}\cos^2\theta_\mathrm{B} - \epsilon^1_{zz}\sin^2\theta_\mathrm{B}$ for $p$-polarization. The optical dielectric tensor modulation components $\epsilon^1_{xx}$ and $\epsilon^1_{zz}$ are governed by the degree of the phase separation of LC from the polymer and by the dielectric anisotropy $\epsilon_a = \epsilon_\parallel - \epsilon_\perp$ and the distribution of LC molecules within droplets. The ratio $\epsilon^1_{xx}/\epsilon^1_{zz}$ is connected with the mean LC orientation. Higher deviations from 1 suggest higher order in the LC alignment.

From the measured efficiencies $\eta_p$ and $\eta_s$ we can calculate the components

of the dielectric tensor modulation $\epsilon^1_{xx}$ and $\epsilon^1_{zz}$ using Equation (3). The mean refractive index $n_{\mathrm{m}}$ was calculated from the weight fraction of LC and polymer on the basis of the material parameters given by the manufacturer. For the samples from the VIS series, the diffraction efficiency was higher for $p$-polarization, indicating a stronger dielectric modulation in the $x$ direction, i.e. $\epsilon^1_{xx} > \epsilon^1_{zz}$. This means that the LC molecules in the droplet planes are on average oriented parallel to the $x$ axis. Measurements in UV samples showed the opposite behavior ($\epsilon^1_{xx} < \epsilon^1_{zz}$), therefore we may expect that in this case LC molecules are on average oriented parallel to the droplet planes.

The largest of the two tensor components $\epsilon^1_{xx}$ and $\epsilon^1_{zz}$ is taken as a measure of the grating strength. Figure 3 shows the result for $\epsilon^1_{\mathrm{max}}/\epsilon_a$ obtained in VIS and UV samples with different grating spacings. In VIS samples where $\epsilon^1_{\mathrm{max}} =$

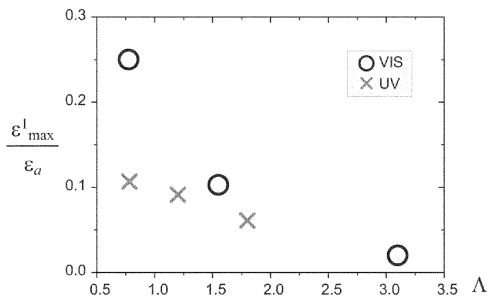


FIGURE 3: The ratio of the maximal dielectric modulation component $\epsilon^1_{\mathrm{max}}$ to the dielectric anisotropy $\epsilon_a$ of the pure LC as a function of the grating spacing measured in the VIS ($\epsilon^1_{\mathrm{max}} = \epsilon^1_{xx}$) and UV ($\epsilon^1_{\mathrm{max}} = \epsilon^1_{zz}$) samples.

$\epsilon^1_{xx}$, BL038 nematic liquid crystal is used which has a dielectric anisotropy of $\epsilon_a = 0.905$ in the bulk. In UV samples where $\epsilon^1_{\mathrm{max}} = \epsilon^1_{zz}$, TL203 nematic liquid crystal is used which has a dielectric anisotropy of $\epsilon_a = 0.656$ in the bulk. For both the compositions, $\epsilon^1_{\mathrm{max}}$ decreases with increasing grating spacing, which is in agreement with SEM images for VIS samples[3], revealing that the spatial modulation of the structure decreases with increasing $\Lambda$. We may therefore expect similar droplet distributions also in the UV samples. In UV samples that contain only the commercial pre-polymer mixture, the modulation $\epsilon^1_{\mathrm{max}}$ is lower than in our VIS samples, that were already optimized with the respect to the

diffraction properties[2].

Figure 4 shows the data for the dielectric anisotropy $\epsilon^1_{xx}/\epsilon^1_{zz}$ in our samples. In all the samples the decrease of the anisotropy with increasing grating spacing is observed. Comparing this observation with SEM images of VIS samples[3] we may expect that the droplet ellipticity is decreased for larger grating spacings. This may result in a less aligned LC orientational profile within the droplets. Despite of the lower modulation, UV cured gratings exhibit a higher modulation

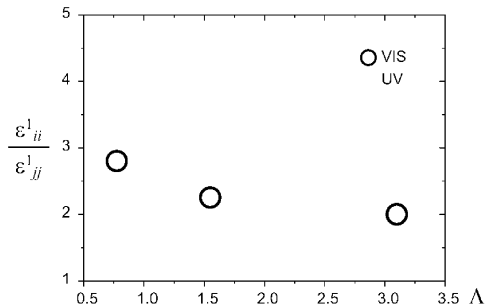


FIGURE 4: The ratio of the dielectric modulation components $\epsilon^1_{ii}/\epsilon^1_{jj}$ as a function of the grating spacing measured in the VIS samples ($\epsilon^1_{ii}/\epsilon^1_{jj} = \epsilon^1_{xx}/\epsilon^1_{zz}$) and in the UV samples ($\epsilon^1_{ii}/\epsilon^1_{jj} = \epsilon^1_{zz}/\epsilon^1_{xx}$) .

anisotropy. Since the uniform distribution of nematic orientations in the grating planes brings a further reduction of 50 % when averaged in the direction of $s$-polarization, we may conclude that droplet ellipticity is much higher in our UV samples compared to VIS samples.

The proposed nematic structures in the droplets forming our samples is schematically shown in Figure 5. In the first case a relatively strong homeotropic anchoring condition implies an axial LC structure oriented along the minor axis of the ellipsoidal droplets. In the second case a weaker homeotropic anchoring implies an axial structure oriented along the major axis of the droplets. In the case of VIS samples the droplets are probably mainly of the minor-axial structure with minor droplet axes parallel to the grating vector. In the case of UV samples we may either have the minor-axial structure but the reversed droplet orientations, i.e. droplet minor axes parallel to the droplet planes, or a different

anchoring condition that implies a major-axial structure in the droplets.

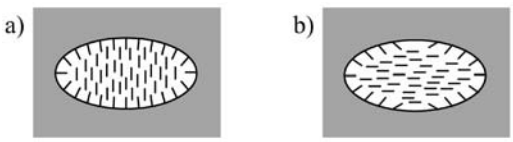


FIGURE 5: The schemes of the nematic structure in ellipsoidal droplets with a) relatively strong homeotropic anchoring (minor-axial structure) and b) weak homeotropic anchoring (major-axial structure).



**Temperature dependence**

In order to obtain additional information on the structure of H-PDLCs and their useful temperature range, we have analyzed the temperature dependence of diffraction properties of different samples in the interval of $20\,^{\circ}\mathrm{C} < T < 100\,^{\circ}\mathrm{C}$. The observed dependencies were qualitatively independent of the grating spacing, so we report only on the data for the two samples of different composition. The results are summarized in Figure 6. Upon heating the efficiencies change due to the transition of the LC from nematic to the isotropic phase, due to possible polymer structural changes, and due to modification of the anchoring strength which affects the director profile within the droplets[6]. Above the nematic-isotropic clearing temperature the value of $\eta_p/\eta_s$ is constant, as determined by the scalar coupled-wave theory for isotropic gratings[4]. The clearing temperature in the bulk BL038 liquid crystal used in VIS samples is 100°C and in TL203 liquid crystal used in UV samples is 77°C. It can be noticed in Figure 6 that the nematic-isotropic transition is at around 60°C in VIS samples and 55 °C in UV samples. The lower values of the nematic-isotropic transition temperature in H-PDLC samples indicate that the LC material in droplets is mixed with other emulsion ingredients.

The behavior of diffraction efficiencies below the clearing temperature significantly deviates from the expected $\epsilon_a(T)$ dependence. In VIS samples with $\eta_p/\eta_s > 1$ at room temperature, there is always a temperature interval below the clearing temperature, in which the ratio of efficiencies is considerably lower

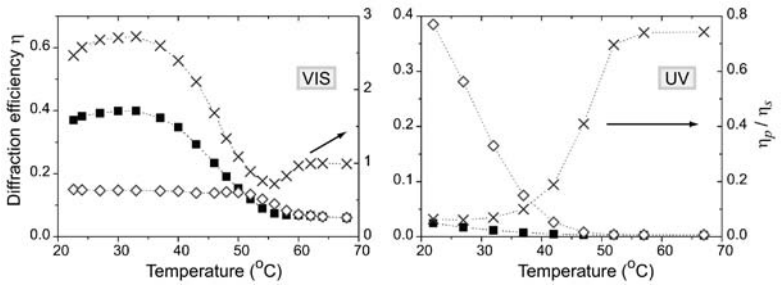


FIGURE 6: The temperature dependence of the diffraction efficiencies for the two characteristic samples, VIS sample with $\Lambda = 1.55$ $\mu$m, and UV sample with $\Lambda = 1.2$ $\mu$m. Solid squares denote diffraction efficiencies for $p$-polarization, open diamonds for $s$-polarization, and crosses for the ratio $\eta_p/\eta_s$.

than above the transition. The inversion of the polarization sensitivity suggests that the director structure in the droplets changes so that the average director is rotated from the direction parallel to the grating vector to perpendicular directions. The effect may be related to the polymer matrix changes and/or the reduction of the anchoring strength. The latter may change the most favorable director structure within the droplets, from the nematic structure illustrated in Figure 5a to the structure illustrated in Figure 5b. In UV samples the average director orientation remains unchanged with increasing temperature. As already mentioned, the reversed polarization sensitivity of UV samples at room temperature could be interpreted with the rotated droplet orientations with respect to the droplet planes. The observed temperature dependence, however, disproves this assumption as otherwise the polarization dependence should be reversed before the transition. The anchoring in UV samples is therefore very weak already at room temperature, which results in the reversed LC structure in the droplets (Figure 5b) in these samples.

## CONCLUSIONS

We performed comparative experimental investigations of switchable PDLC gratings of different compositions and grating spacings. The LC orientational order was found to be much higher in UV cured samples than in VIS samples, resulting in a high polarization sensitivity. The LC orientational structure in the droplets was found to be mostly axial-like. The orientational order and the separation between polymer and LC droplet planes was found to be higher for smaller grating spacings. The observed temperature dependencies of diffraction efficiencies in VIS samples revealed structural changes which are presumably related to the modification of the anchoring strength with temperature.

### *References*

[1] R. L. Sutherland, L. V. Natarajan, T. J. Bunning, and V. P. Tondiglia, in Handbook of Advanced Electronic and Photonic Materials and Devices, edited by H. S. Nalwa (Academic Press, New York, 2001), pp. 67-103.

[2] C. C. Bowley and G. P. Crawford, Appl. Phys. Lett. **76**, 2235 (2000).

[3] M. Jazbinšek, I. Drevenšek Olenik, M. Zgonik, A. K. Fontecchio, and G. P. Crawford, J. Appl. Phys. **90**, 3831 (2001).

[4] H. Kogelnik, Bell Syst. Tech. J. **48**, 2909 (1969).

[5] G. Montemezzani and M. Zgonik, Phys. Rev. E **55**, 1035 (1997).

[6] K. Amundson, Phys. Rev. E **53**, 2412 (1996).